



Research Article

The Activated Carbon from Walnut Shell Using CO₂ and Methylene Blue Removal

İlhan KÜÇÜK¹, Yunus ÖNAL², Canan AKMİL BAŞAR²

¹ Department of Chemistry, Faculty of Art and Science, Inonu University, 44280 Malatya, Turkey, kckilhan@gmail.com orcid.org/0000-0003-2876-3942

² Department of Chemical Engineering, Faculty of Engineering, Inonu University, 44280 Malatya, Turkey, yunus.onal@inonu.edu.tr, orcid.org/0000-0001-6342-6818

Department of Chemical Engineering, Faculty of Engineering, Inonu University, 44280 Malatya, Turkey, canan.basar@inonu.edu.tr, orcid.org/0000-0003-3574-0773

ARTICLE INFO

Article history:

Received 27 October 2020
Received in revised form 28
December 2020
Accepted 28 December 2020
Available online 30 March 2021

Keywords:

*Biomass, Carbonization, Physical
activation, Activated carbon.*

ABSTRACT

In this study, activated carbon with strong adsorption property was synthesized from lignocellulosic structured walnut shell. Active carbon synthesis was realized in two stages: carbonization and physical activation. Carbonization was carried out at eight different temperatures (300-1000°C), 500 mL/min N₂ gas flow and 10°C/min heating rate for 1 hour. Activation was done at two different temperatures (800-900 °C) at 100 ml/min CO₂ gas flow for 1 hour. Characterization of activated carbons was carried out and their adsorption capacities were examined with methylene blue. The surface areas of the activated carbons were investigated by BET analysis and the surface areas ranged from 56,79 to 652,22 m²/g. Amounts of micro and mesoporous in these surface areas were calculated. Besides, SEM analysis indicates the porous structure and XRD analysis confirms that the structure is amorphous. Methylene blue adsorption was performed in the aqueous phase and the capacities of the activated carbons were calculated. The methylene blue adsorption capacity of activated carbons varies between 15,96 -174,81 mg/g.

Doi: 10.24012/dumf.816317

* Corresponding author
Yunus ÖNAL
✉ e-mail: yunus.onal@inonu.edu.tr

Introduction

Activated carbons are one of the most widely used adsorbents due to their high surface areas and pores [1]. Even if it has many applications such as energy storage [2], purification [3], water treatment [4], pharmaceutical [5], chemical and petroleum industries [6], separation, catalysis [7], nuclear power stations [8], electrodes for electric double-layer capacitors [9], batteries, fuel cells [10], hydrometallurgy [11], it is preferable in adsorption because it is cheaper than other adsorbents and thanks to the diversity in raw material usage, the importance of activated carbon are increasing every year [12].

One of the most important applications of active carbons is the adsorption of liquid-phase organic and inorganic compounds [13]. In addition, the use of activated carbon in the purification of polluted waters and groundwater is increasing [14]. Activated carbons are used in pre-treatments of purification processes or advanced purification. Adsorption in liquid phase applications results from the interaction of adsorbed material and activated carbon. An electrostatic interaction with activated carbon occurs when the adsorbed substance is an electrolyte. The push and pull forces in these electrostatic interactions vary with the electron charge on the surface of the activated carbon, the chemical structure of the substance to be adsorbed, and the ion charge in the solution. In non-electrolyte fluids, these interactions occur via Van der Waals interactions, hydrophobic, hydrophilic interactions and hydrogen bonds [15].

Activated carbon synthesis was generally synthesized from coal, lignite, wood and animal bones in ancient times. Nowadays, these products are not preferable because they are expensive and not renewable. These products have been replaced by agricultural products and their wastes. Some of these wastes are pistachio-nut [16], hazelnut shell [17], corn cob [18], bamboo [19], pruning mulberry shoot [20], olive stone [21], Jojoba seed [22], coconut shell [23], Jatropha husk [24], hazelnut bagasse [25], Chinese fir sawdust [26] and many others. When activated carbon synthesis is made from these

products, the yield is lower than that produced from coal and lignite. This is because the amount of carbon in these products is less than others.

The synthesis of activated carbon is generally carried out in two ways: carbonization and activation. Activation is usually realized in two different ways: physical and chemical activation [27]. However, physicochemical activation has also emerged in recent years [28]. Chemical activation can be done by mixing the sample with the chemical substance after carbonization or by placing the chemical substance on the raw sample. In case chemical substance is placed on raw sample, activated carbon synthesis is performed in one step by passing carbonization step. In both cases, the atmosphere is made inertly with N_2 gas. Chemicals commonly used in chemical activation are $ZnCl_2$, H_3PO_4 [29], H_2SO_4 , K_2S , $KCNS$ [25], HNO_3 , H_2O_2 , $KMnO_4$, $(NH_4)_2S_2O_8$ [30], $NaOH$, KOH [31], and K_2CO_3 [32]. In physical activation, the sample is carbonized in an inert atmosphere (with N_2 gas). After carbonization, the sample which is subjected to physical activation is usually exposed to CO_2 , water vapor, CO_2 -water vapor mixture or CO_2 -air mixture and the activation process is completed.

In physicochemical activation, activated carbon synthesis is made by placing a chemical agent either on the raw sample or on the carbonized material and placed in the gas atmosphere used in physical activation. It is a kind of mixture of chemical and physical activation [28]. Activated carbons expand the surface areas thanks to the pores on their surfaces. These pores are generally defined in three different ways: Micropores (<2nm), mesopores (2< >50 nm) and macropores (>50 nm) [12].

Biomasses with lignocellulosic structure are suitable materials for active carbon synthesis. Since these biomasses are both renewable and cheap, they can be used continuously in the synthesis of activated carbon [15]. Additionally, since these materials are inexpensive to store, biomasses are suitable for activated carbon synthesis. Lignocellulosic structures consist of three basic units: cellulose, hemicellulose, and lignin. These units decompose with temperature and form a porous structure [12].

In this study, activated carbon synthesis was performed in different conditions from walnut shell and properties of these activated carbons were investigated. The decrease in the amount of methylene blue in the aqueous phase was investigated by making use of adsorption which is one of the most used fields.

Materials and Methods

Preparation of the Samples

The supplied walnut shell (Malatya, Hekimhan region) was weighed approximately 325 g without any pre-treatment and placed in a three-zone oven.

Carbonization

Walnut shells were placed at Protherm PZF 12/50/700 model 3-zone furnace at eight different temperatures (300, 400, 500, 600, 700, 800, 900, 1000 ° C) with 10 °C/min heating under 500 mL/min N₂ gas flow for 60 min. The liquid yield was calculated by means of the back cooler and the collecting vessel attached to the furnace outlet and the gas yield was calculated from the difference.

Physical Activation

The carbonized materials were activated through a 3-zone furnace model Protherm PZF 12/60/600. CO₂ was used during the activation process and the gas flow was set to 100 mL/min. The process was operated at two different temperatures (800, 900 ° C) and activated for 1 hour with a heating rate of 10 ° C.

Preparation of Methylene Blue

The methylene blue was placed in a petri dish and placed in a furnace at 105 °C for 1 day. 1 grams of methylene blue was weighed with precision scales, and 1000 ppm stock solution was prepared.

Adsorption

100 mL methylene blue solution which is diluted from 1000 ppm stock solution to 200 ppm, was placed in 200 mL conical flasks and 0,1 grams of activated carbon added to the flask under magnetic stirring. The flasks were sealed and mixed for 24 hours. After 24 hours, the samples

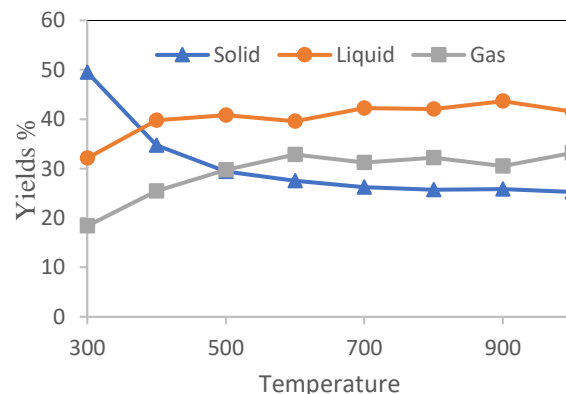
were filtered through syringe tip filters and analyzed using UV-VIS analyzer at 660 nm.

Analysis

The surface area of activated carbon samples determined on Micromeritics TriStar 3000, XRD measurements were realized using Japanese Rigaku Rad B-DMAX II (Cu K-alpha) instrument, SEM measurements were carried out using Leo EV040 scanning electron microscope and element analyze were done with CHNS- 932 (LECO) Elemental Analyzer.

Results and Discussion

Biomasses transform into 3 different forms as solid, liquid and gas when exposed to heat under an inert atmosphere. Solid, liquid and gas transformations of walnut shells with temperature are shown in Figure 1. The percentages of solid, liquid and gas form were calculated and plotted from Figure 1. According to the graphic, the amount of the solid product decreases with increasing temperature while the amount of the liquid and gas product generally increased. The decrease in the solid product occurred rapidly up to 600°C and after 600°C, this reduction almost stopped. The highest solid yield was seen at 300°C as expected. Although there is no regular increase in liquid and gas yields, there is generally an increment. The highest liquid yield was achieved at 900°C. Liquid yield decreases again after 900°C. The gas yield is highest at 600°C where the increment is not common overall.



There is a decrease after 600 °C.

Figure 1: Solid (char), liquid and gas yields of carbonized samples.

Table 1: BET analysis of activated carbon

Code	Carbonization	Physical Activation	S_{BET} m ² /g	S_{micro} %	S_{meso} %	V_T cm ³ /g	V_{micro} cm ³ /g	V_{mezo} cm ³ /g	dp nm
	Temperature (°C/ 500 mL/dk N ₂)	Temperature (°C/100 mL CO ₂)							
AC1	300	800	369,24	97,12	2,88	-	0,188	-	-
AC2	300	900	629,13	81,52	18,48	0,343	0,273	0,070	2,182
AC3	400	800	425,16	86,21	13,79	0,239	0,192	0,047	2,256
AC4	400	900	516,86	86,41	13,59	0,286	0,235	0,051	2,218
AC5	500	800	382,93	88,01	11,99	0,215	0,177	0,038	2,252
AC6	500	900	652,22	82,42	17,58	0,365	0,284	0,081	2,238
AC7	600	800	387,04	88,78	11,22	0,215	0,180	0,035	2,225
AC8	600	900	584,94	78,6	21,4	0,324	0,243	0,081	2,221
AC9	700	800	380,97	95,43	4,57	0,200	0,191	0,008	2,103
AC10	700	900	557,20	85,21	14,79	0,305	0,250	0,055	2,196
AC11	800	800	411,74	92,5	7,5	0,213	0,200	0,013	2,077
AC12	800	900	644,31	83,77	16,23	0,350	0,285	0,065	2,177
AC13	900	800	320,01	100	-	-	0,173	-	-
AC14	900	900	564,52	84,18	15,82	0,306	0,251	0,055	2,173
AC15	1000	800	56,79	100	-	-	0,07	-	-
AC16	1000	900	400,42	94,54	5,46	0,19	0,19	-	1,97

BET analysis of the synthesized activated carbons is shown in Table 1. The highest surface area seen in Table 1 is 652,22 m²/g. According to Table 1, changes in carbonization temperature caused changes in the surface area. Although the elevation of the carbonization temperature causes a partial increase in the surface area, there is a decrease in the surface area after a certain temperature [33]. The effect belongs mostly to the activation conditions. It is seen that the surface area increases with the increase of activation temperature in samples obtained at the same carbonization temperature. The increased activation temperature increases the kinetic energy of the gas used during activation, further

impacting the carbonized product, causing the surface area of the activated carbon to widen [34]. These phenomena partly explains the increase in the surface area. In addition, two types of pores which are micro and mesopores were found in activated carbon with the increased surface area. Increased activation temperature leads to an increase in the amount of micropore and mesopore which is common in all samples. Besides, it is seen that the percentage of micropore decreases in all samples and the percentage of mesopore increases with increasing activation temperature. Increased temperature positively affected mesopore formation of all samples. Looking at the total volumes of the

synthesized activated carbons, it is possible to observe the effect of the activation temperature. There is an increase in the total volumes as a result of the activation temperature increase. This increment can be observed both in micro and meso volumes. The average pore diameter is about 2 nm in all samples.

N_2 adsorption isotherm of different activated carbons is given in Figure 2. According to the classification of the IUPAC (International Union of Pure and Applied Chemistry), all activated carbons have type I hybrid shape isotherms. In such isotherms, N_2 adsorption rapidly increases at low P/P_0 pressures, then this rapidly increases slow and remains constant. Such activated carbons are generally activated carbons with the low surface area, narrow pore diameters, and high micropore content. Table 1 show that the amount of micropore is high. The graph shows an increase in the last sections, in the regions where P/P_0 is approaching 1, and it can be shown as a proof that there is a small amount of mesopore in this structure.

The pore distribution graphs of different activated carbons were calculated by the BJH method and given in Figure 3. As shown in this graph, pore diameters are usually around 2 nm and the amount of micropore is greater than the amount of mesopore. These results confirm the BET results in Table 1 and the N_2 adsorption results in Figure 2.

Another important method of analysis for activated carbons is SEM images. SEM images of some activated carbons are shown in Figure 4. Porous structure formation can be seen in the synthesized activated carbons as SEM images shows.

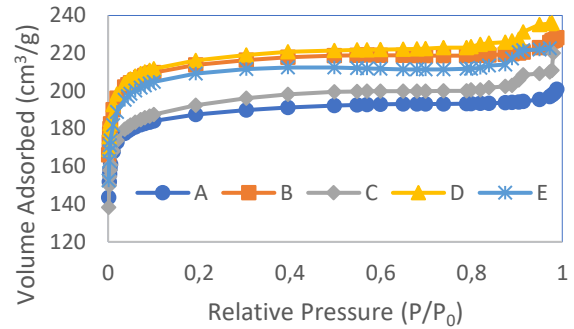


Figure 2. Adsorption isotherms of N_2 . A. AC14. B. AC12. C. AC8. D. AC6. E. AC2.

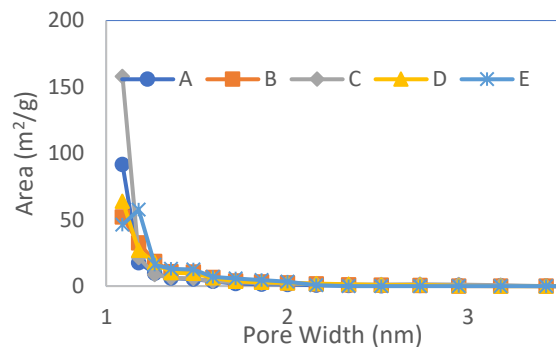
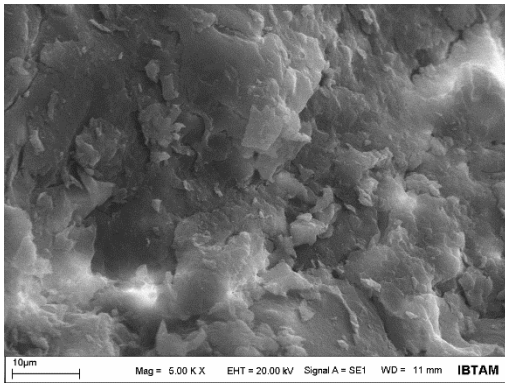
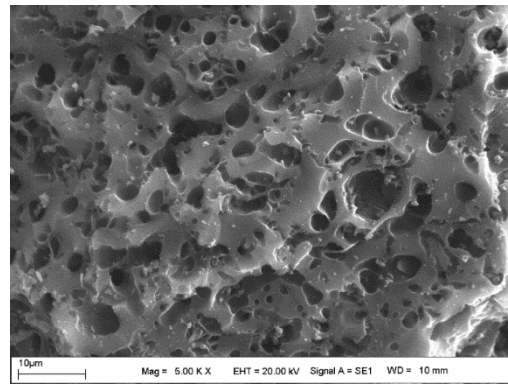


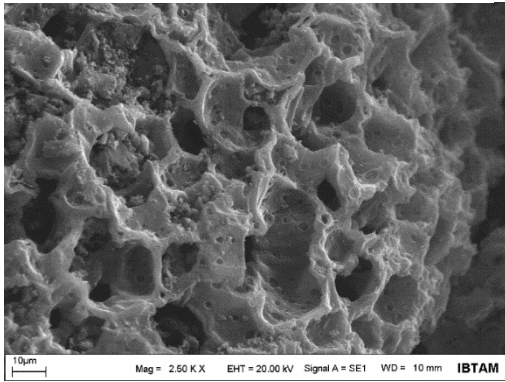
Figure 3. Pore size distribution of activated carbon sample. A. AC14. B. AC12. C. AC8. D. AC6. E. AC2.



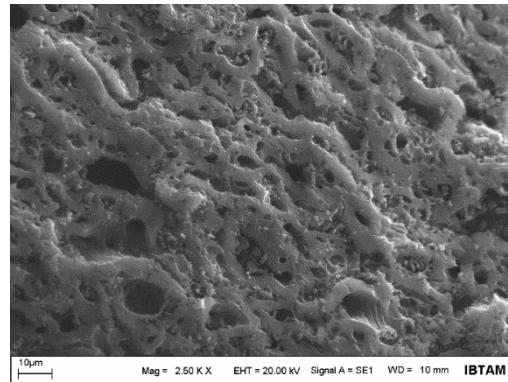
A



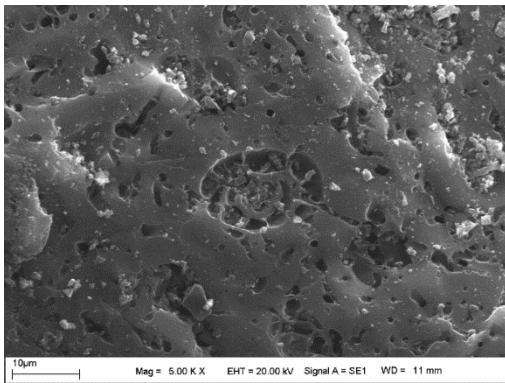
B



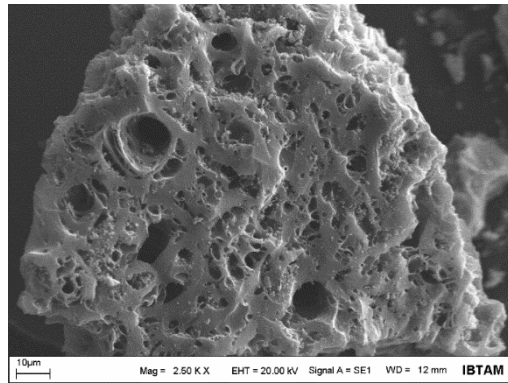
C



D



E



F

Figure 4. A. SEM image of raw walnut shell. B. AC6. C. AC2. D. AC14. E. AC12. F. AC8.

Figure 5 shows the results of the XRD analysis of activated carbons. The raw material used has a less organized structure that does not show any specific crystalline structure indication, probably due to the various organic impurities and volatile substances present in the structure. When XRD results are considered, there is no crystal region in the structure of activated carbon and the structure is amorphous. In particular, the peak observed at about 23° in raw material analysis generally belongs to the cellulose peak seen in cellulose-based materials. The FTIR spectrum was used to determine the surface chemical groups of the raw material and some activated carbons and the results are given in Figure 6. Characteristic lignocellulosic structure peaks can be seen at the raw material spectrum. These peaks, approximately 3500 cm^{-1} the peak OH is caused by stress vibration and occurs in phenolic or alcohol groups. These groups are generally present in the structure of glycosidic chains. Also, the peak in the spectrum of approximately 2900 cm^{-1} C-H asymmetric and symmetrical vibration peaks are caused by the methylene groups, such as $-\text{CH}_2$. The peak seen at about 1700 cm^{-1} originates from carbonyl groups ($\text{C}=\text{O}$) and comes from ester, ketones and carboxylic acids. The peak at about 1600 cm^{-1} belong to the $\text{C}=\text{C}$ bond vibration of alkenes. The peak at approximately 1450 cm^{-1} is due to the stretching vibrations of the ether groups in the stevioside structure. The peak around 1260 cm^{-1} belongs to the stretching vibration of ester groups. Finally, the peak at about 1000 cm^{-1} is the vibrations caused by C-OH and C-O-C bonds. When the FTIR spectra of the activated carbons were compared with the raw material, these peaks either disappeared or decreased in intensity.

Table 2 shows the element analysis of all activated carbons and element analysis of the raw material. According to the analysis results, the amount of carbon increases in all activated carbons compared to raw materials. Besides, there is a decrease in the amount of hydrogen and an increase in the amount of nitrogen. No sulphur was detected in activated carbons except for only one sample.

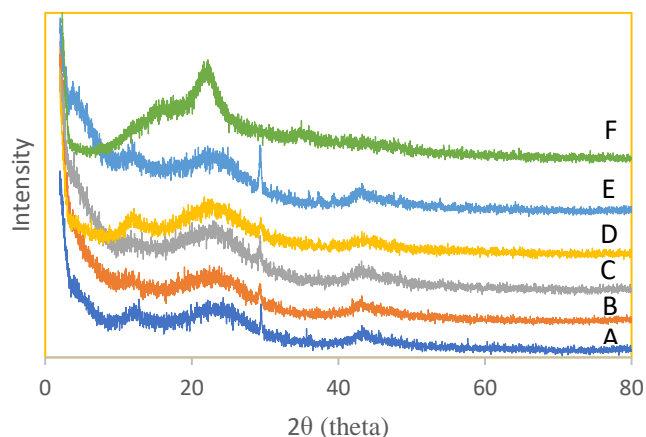


Figure 5. XRD chart of samples A. AC14. B. AC12. C. AC8. D. AC6. E. AC2. F. XRD chart of walnut Shell

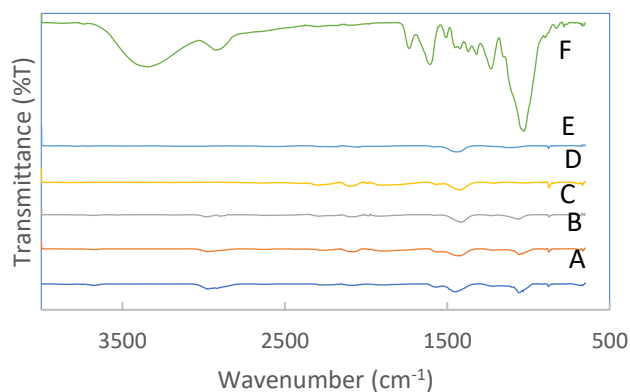


Figure 6. FTIR spectrum of raw material and activated carbon samples A. AC14. B. AC12. C. AC8. D. AC6. E. AC2. F. FTIR spectrum of raw material

Table 2: Elemental analysis of activated carbon.

Carbonization		Physical Activation			
Temperature (°C/500 mL/dk N ₂)	Temperature (°C/100 mL CO ₂)	C	H	N	S
	Raw Material	48,74	5,664	0,149	-
300	800	64,80	1,170	0,237	-
300	900	43,12	0,611	-	0,094
400	800	88,21	1,232	0,220	-
400	900	70,03	0,874	0,204	-
500	800	86,48	1,324	0,245	-
500	900	84,19	1,120	-	-
600	800	71,18	1,210	0,228	-
600	900	76,71	0,605	-	-
700	800	53,84	1,031	0,156	-
700	900	67,89	0,935	0,213	-
800	800	73,77	0,983	0,287	-
800	900	72,13	1,261	0,182	-
900	800	65,91	0,884	0,345	-
900	900	54,00	0,988	0,164	-
1000	800	62,22	0,660	0,655	-
1000	900	72,35	0,779	0,339	-

One of the important points during the adsorption process is the length, width and thickness of the molecule to be adsorbed. If the molecule to be adsorbed is too large to pass through the pores of the synthesized activated carbons, adsorption does not occur or takes place very little. Therefore, the adsorbent used in adsorption studies is important.

The methylene blue molecule used in this study is length, width and width of 1.43, 0.61 and 0.4 nm, respectively. It is shown in Table 1 that the average pore diameters of the synthesized active carbons are greater than the methylene blue molecule. Therefore, adsorption was realized.

In this study, the removal of impurities in aqueous solutions, which is one of the application fields of activated carbons, was carried out with methylene blue, and the adsorption capacity of methylene blue was determined. The methylene blue adsorption capacities of the activated carbons are shown in Table 3. Adsorption capacity increased in increasing surface areas generally. The highest surface area is 652 m²/g. However, the highest adsorption capacity is seen for activated carbon with a surface area of 644 m² / g. The reason for this is that this activated carbon has a higher micropore pore area (83.77%) compared to the other.

Table 3: Methylene blue adsorption capacity of activated carbon.

Carbonization	Physical Activation		
Temperature (°C/500 mL/dk N ₂)	Temperature (°C/100 mL CO ₂)	S _{BET} m ² /g	Adsorption Capacity q _e (mg/g)
300	800	369,24	23,99
300	900	629,13	154,46
400	800	425,16	45,55
400	900	516,86	65,68
500	800	382,93	26,19
500	900	652,22	155,45
600	800	387,04	40,93
600	900	584,94	149,62
700	800	380,97	16,29
700	900	557,20	96,51
800	800	411,74	39,5
800	900	644,31	174,81
900	800	320,01	24,1
900	900	564,52	132,02
1000	800	56,79	15,96
1000	900	400,42	55,45

Adsorption capacity was calculated according to equation 1.

$$q_e = \frac{C_0 - C}{W} \times V \quad (\text{Eq.1})$$

where C_0 and C (mg L⁻¹) are the initial and equilibrium liquid phase concentrations of MB, respectively, V (L) is the volume of the solution, and W (g) is the mass of dry adsorbent used.

Conclusions

In this study, the changed parameters in the experiments caused changes in the surface areas of the activated carbons. The changing carbonization and activation temperatures caused a change in the type and amount of pores formed in the activated carbon. Activated carbon has the highest surface area was collected at 500 ° C carbonization and 900°C activation temperature.

Additionally, the increased activation temperature had a positive effect on the surface area but caused a decrease in the percentage of micropore. If it is desired to keep the amount of micropores in the structure excess, a low activation temperature should be used. Since chemical activation is generally used in previous

studies, the surface areas of those activated carbons are higher than this study. Active carbon synthesized by chemical activation has less micropore, while the amount of mesopore is high. At this point, it is clear that the activation used in the synthesis of activated carbon is important. As a result, physical activation with the CO₂ can be used in a study aimed to increase the amount of micropore. In addition, that, the pore distributions of the formed activated carbons will vary on a smaller scale.

Acknowledgments: This study was supported by the unit of Scientific Researches of Inonu University in Malatya, Turkey; Project No: FDI-2017-680

REFERANSLAR

1. Fulazzaky MA, Omar R (2012) Removal of oil and grease contamination from stream water using the granular activated carbon block filter *Clean Technologies and Environmental Policy* 14: pp.965-971
2. Shi K, Ren M, Zhitomirsky I (2014) Activated carbon-coated carbon nanotubes for energy storage in supercapacitors and capacitive water purification *ACS Sustainable Chemistry Engineering* 2: pp.1289-1298
3. Ao C, Lee S (2005) Indoor air purification by photocatalyst TiO₂ immobilized on an activated carbon filter installed in an air cleaner *Chemical engineering science* 60: pp.103-109
4. Bhatnagar A, Hogland W, Marques M, Sillanpää M (2013) An overview of the modification methods of activated carbon for its water treatment applications *Chemical Engineering Journal* 219: pp.499-511
5. Baccar R, Sarrà M, Bouzid J, Feki M, Blánquez P (2012) Removal of pharmaceutical compounds by activated carbon prepared from agricultural by-product *Chemical engineering journal* 211: pp.310-317
6. Anirudhan T, Sreekumari S, Bringle C (2009) Removal of phenols from water and petroleum industry refinery effluents by activated carbon obtained from coconut coir pith *Adsorption* 15:439
7. Heidenreich RG, Krauter JG, Pietsch J, Köhler K (2002) Control of Pd leaching in Heck reactions of bromoarenes catalyzed by Pd supported on activated carbon *Journal of Molecular Catalysis A: Chemical* 182: pp.499-509
8. Matsuo T, Nishi T (2000) Activated carbon filter treatment of laundry waste water in nuclear power plants and filter recovery by heating in vacuum *Carbon* 38: pp.709-714
9. Hasegawa G (2013) Monolithic electrode for electric double-layer capacitors based on macro/meso/microporous S-containing activated carbon with high surface area. In: *Studies on Porous Monolithic Materials Prepared via Sol-Gel Processes*. Springer, pp 79-89.
10. Bai Y, Liu Y, Tang Y, Xie Y, Liu J (2011) Direct carbon solid oxide fuel cell—a potential high performance battery *international journal of hydrogen energy* 36: pp.9189-9194
11. Abbruzzese C, Fornari P, Massidda R, Vegliò F, Ubaldini S (1995) Thiosulphate leaching for gold hydrometallurgy *Hydrometallurgy* 39: pp.265-276
12. Yahya MA, Al-Qodah Z, Ngah CZ (2015) Agricultural bio-waste materials as potential sustainable precursors used for activated carbon production: A review *Renewable Sustainable Energy Reviews* 46: pp.218-235
13. Radovic LR, Moreno-Castilla C, Rivera-Utrilla J (2001) Carbon materials as adsorbents in aqueous solutions. *Chemistry physics of carbon*.
14. Meidl J (1997) Responding to changing conditions: how powdered activated carbon systems can provide the operational flexibility necessary to treat

- contaminated groundwater and industrial wastes Carbon 35: pp.1207-1216
15. Dias JM, Alvim-Ferraz MC, Almeida MF, Rivera-Utrilla J, Sánchez-Polo M (2007) Waste materials for activated carbon preparation and its use in aqueous-phase treatment: a review Journal of environmental management 85: pp.833-846
 16. Lua AC, Yang T (2005) Characteristics of activated carbon prepared from pistachio-nut shell by zinc chloride activation under nitrogen and vacuum conditions Journal of colloid interface science 290: pp.505-513
 17. Örkün Y, Karatepe N, Yavuz R (2012) Influence of temperature and impregnation ratio of H₃PO₄ on the production of activated carbon from hazelnut shell Acta Physica Polonica-Series A General Physics pp.121:277
 18. Tsai W-T, Chang C, Lee S (1998) A low cost adsorbent from agricultural waste corn cob by zinc chloride activation Bioresource Technology 64: pp.211-217
 19. Ademiluyi F, Amadi S, Amakama NJ (2009) Adsorption and Treatment of Organic Contaminants using Activated Carbon from Waste Nigerian Bamboo Journal of Applied Sciences Environmental Management 13(3), pp.39-47
 20. Wang J, Wu F, Wang M, Qiu N, Liang Y, Fang S, Jiang X (2010) Preparation of activated carbon from a renewable agricultural residue of pruning mulberry shoot African Journal of Biotechnology 9: pp.2762-2767
 21. Spahis N, Addoun A, Mahmoudi H, Ghaffour N (2008) Purification of water by activated carbon prepared from olive stones Desalination 222: pp.519-527
 22. Tawalbeh M, Allawzi M, Kandah MI (2005) Production of activated carbon from jojoba seed residue by chemical activation residue using a static bed reactor Journal of Applied Sciences 5: pp.482-487
 23. Yusufu M, Ariahu C, Igbabul B (2012) Production and characterization of activated carbon from selected local raw materials African Journal of Pure Applied Chemistry 6: pp.123-131
 24. Ramakrishnan K, Namasivayam CJJEEM (2009) Development and characteristics of activated carbons from Jatropha husk, an agro industrial solid waste, by chemical activation methods J Environ Eng Manage 19: pp.173-178
 25. Demiral H, Demiral I, Tümsek F, Karabacakoğlu B (2008) Pore structure of activated carbon prepared from hazelnut bagasse by chemical activation Surface Interface Analysis 40: pp.616-619
 26. Qiu K, Yang S, Yang J (2009) Characteristics of activated carbon prepared from Chinese fir sawdust by zinc chloride activation under vacuum condition Journal of Central South University of Technology
 27. Jutakridsada P, Prajaksud C, Kuboonya-Aruk L, Theerakulpisut S, Kamwilaisak K (2016) Adsorption characteristics of activated carbon prepared from spent ground coffee Clean Technologies and Environmental Policy 18: pp.639-645
 28. Oubagaranadin J, Murthy Z (2011) Activated carbons: Classifications, properties and applications.
 29. Donald J, Ohtsuka Y, Xu CC (2011) Effects of activation agents and intrinsic minerals on pore development in activated carbons derived from a Canadian peat Materials Letters 65: pp.744-747
 30. Al-Qodah Z, Shawabkah R (2009) Production and characterization of granular activated carbon from activated sludge Brazilian Journal of Chemical Engineering 26: pp.127-136
 31. Gu Z, Wang X (2013) Carbon materials from high ash bio-char: a nanostructure

- similar to activated graphene Am Trans Eng Appl Sci 2: pp.15-34
32. Adinata D, Daud WMAW, Aroua MK (2007) Preparation and characterization of activated carbon from palm shell by chemical activation with K_2CO_3 Bioresource technology 98: pp.145-149
33. Daud WMAW, Ali S.W, Sulaiman MZ (2000) The effects of carbonization temperature on pore development in palm shell based activated carbon Carbon 38 : pp.1925-1932
34. Chang CF, Chang CY, Tsait WT, (2000) Effects of burn off and activation temperature on preparation of activated carbon from corn cob agrowaste by CO_2 and steam Journal of Colloid and Interface Science 232: pp.45-49